

See discussions, stats, and author profiles for this publication at: <https://www.researchgate.net/publication/237841822>

Covalent Triazine Frameworks Prepared from 1,3,5-Tricyanobenzene

ARTICLE in CHEMISTRY OF MATERIALS · MAY 2013

Impact Factor: 8.35 · DOI: 10.1021/cm303751n

CITATIONS

48

READS

103

5 AUTHORS, INCLUDING:



Michael Janus Bojdys

Charles University in Prague

20 PUBLICATIONS 680 CITATIONS

SEE PROFILE



Jens Weber

Hochschule Zittau/Görlitz

68 PUBLICATIONS 1,897 CITATIONS

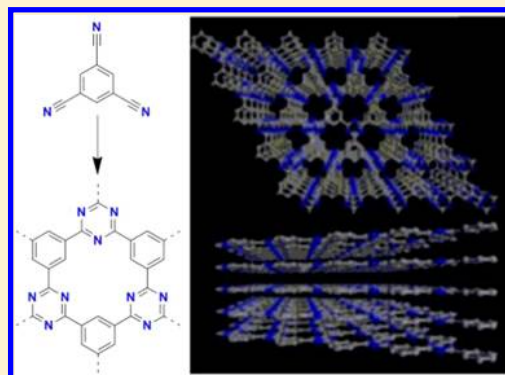
SEE PROFILE

Covalent Triazine Frameworks Prepared from 1,3,5-Tricyanobenzene

Phisan Katekomol,[†] Jérôme Roeser,^{†,‡} Michael Bojdys,[§] Jens Weber,[‡] and Arne Thomas*,[†][†]Department of Chemistry, Functional Materials, Technische Universität Berlin, Hardenbergstrasse 40, Berlin, Germany[‡]Department of Colloid Chemistry, Max Planck Institute of Colloid and Interfaces, Am Mühlenberg 1, 14424 Potsdam/Golm, Germany[§]Department of Chemistry and Centre for Materials Discovery, University of Liverpool, Crown Street, Liverpool, U.K.

S Supporting Information

ABSTRACT: A novel covalent triazine framework (CTF-0) was prepared by trimerization of 1,3,5-tricyanobenzene in molten ZnCl₂. The monomer/ZnCl₂ ratio, the reaction time, and temperature significantly influence the structure and porosity of such networks. XRD measurements revealed that crystalline frameworks can be formed with surface areas around 500 m²·g⁻¹ and high CO₂ uptakes. Increasing the reaction temperature yielded an amorphous material with an enlarged surface area of 2000 m²·g⁻¹. This material showed good catalytic activity for CO₂ cycloaddition.



KEYWORDS: covalent organic framework, microporous polymers, carbon dioxide sorption/utilization, heterogeneous catalysis, organic carbonates

■ INTRODUCTION

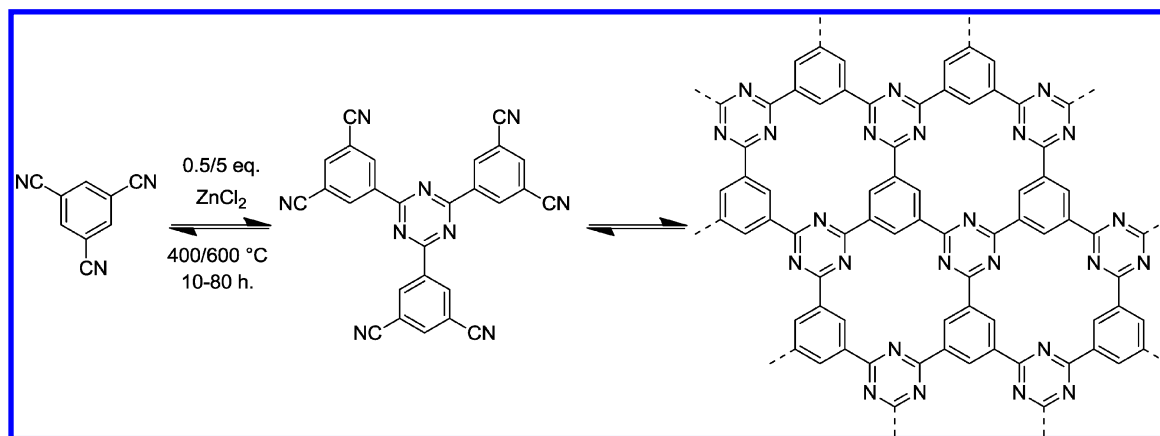
Microporous materials have found various applications of technical relevance such as in separation, gas storage, and catalysis.¹ The invention of synthetic zeolites or the related zeotype materials has largely contributed to the success story of these materials. Besides purely inorganic materials, in recent years, organic–inorganic-hybrid and organic porous materials have been developed and are now actively investigated in fundamental research, with the hope that one day they can complement their inorganic counterparts in certain applications. Especially the introduction of metal–organic frameworks (MOFs)^{2–4} had an enormous impact on the scientific community and has developed to one of the major research fields of material chemistry in the past decade. Porous, covalently bound, and fully organic polymers are another example of emerging materials.^{5–7} These materials have some certain advantages, such as lightweight or ease of functionalization. To introduce permanent porosity into an entirely organic network is challenging due to the “soft” nature of the material, yielding often pore collapse simply by structural deformation due to capillary pressure.^{8,9} Nevertheless, just recently more and more purely organic materials with small pores have been presented, e.g. hypercrosslinked polymers,^{10,11} polymers of intrinsic microporosity,^{5–7,12–17} and covalent organic frameworks^{18–21} were introduced, and a fast increasing amount of novel structures, synthetic schemes, and applications for this class of porous materials were reported.

Covalent organic frameworks (COFs) are a special class of microporous polymer networks as they exhibit a regular architecture and periodic pore structure, thus they are crystalline materials. The key parameter allowing the formation of crystalline structures in covalent chemistry is the reversibility of the reaction pathway, allowing the building blocks to organize into the thermodynamically stable, i.e. crystalline, instead of the kinetically controlled, i.e. amorphous, products.²² The synthesis of a crystalline porous organic framework thus has to be carried out in thermodynamically controlled reactions which was first possible by applying the highly dynamic condensation reaction of boronic acids.¹⁸ After the advent of COF-1, many more COFs with different structures, both 2D and 3D, porosity, and different functionalities based on different starting monomers have been synthesized.^{23–29}

Covalent triazine frameworks (CTFs)^{30–33} are a special and emerging class of COFs. These materials are formed by the trimerization reaction of carbonitriles to form triazine rings. The first reported CTF, CTF-1,³⁰ prepared from 1,4-dicyanobenzene, is thus isoelectronic to COF-1, while the triazines in the former are thermally and chemically much more stable than the boroxine rings in the latter. In consequence much harsher reaction conditions have to be applied to enable the reversible formation of triazines. CTFs are conventionally

Received: November 20, 2012

Revised: February 19, 2013

Scheme 1. Schematic Illustration of the Trimerization of 1,3,5-Tricyanobenzene in Molten ZnCl_2 

synthesized by ionothermal trimerization of carbonitrile groups in molten ZnCl_2 which acts as both solvent and catalyst at temperatures starting from $400 \text{ }^\circ\text{C}$.³⁰ In principle the structures and functionalities of these materials can be easily adjusted by carefully choosing structure-directing monomers as building blocks. Ionothermal synthesis however also imposes some restrictions to the design of such structures. The monomer must be able to endure the temperature of at least $400 \text{ }^\circ\text{C}$ in molten ZnCl_2 which is also a strong Lewis acid. Consequently, so far, only two microporous crystalline CTFs have been reported using this approach namely CTF-1 and CTF-2 based on 1,4-dicyanobenzene and 2,6-dicyanonaphthalene monomers, respectively.^{30,34} In contrast, applying other monomers, higher reaction temperatures or increasing ZnCl_2 /monomer ratios yield amorphous materials, showing sometimes exceptional high surface areas³² which have found interesting applications for example in catalysis.^{35–39} Recently it was shown that crystalline CTFs could also be prepared using trifluorosulfonic acid under microwave irradiation, an approach which has the potential to largely extend the scope of these materials.⁴⁰

In this work, we attempt the synthesis of a novel microporous, crystalline CTF based on 1,3,5-tricyanobenzene (TCB) as monomer under ionothermal conditions. Although an amorphous network based on this monomer has already been reported before in our group,³³ it was very likely that also a crystalline phase can be prepared due to the geometry of the monomer by carefully adjusting the polymerization conditions. As seen in Scheme 1 an ideal reversible polymerization of this monomer would result in a frameworks structure with a smaller pore size and unit cell as observed for CTF-1 and CTF-2, and therefore the material was named “CTF-0”. In addition, such a material should feature higher nitrogen content than other reported CTFs, which have been proven useful for catalytic applications of these materials.^{36,39} From the structure shown in Scheme 1 it can be however reasoned that the pores formed within an ideal framework would be rather small and probably not even accessible to nitrogen molecules. Therefore, investigating the apparent surface area of such frameworks prepared under different conditions can yield insight on the contribution of crystalline and amorphous defect structures, respectively, on the finally observed porosity in such CTFs.

EXPERIMENTAL SECTION

Materials and Methods. 1,3,5-Tricyanobenzene (TCB) was used as purchased from Synthon chemicals, and ZnCl_2 ($\geq 98\%$) and epichlorohydrin were used as purchased from Sigma-Aldrich. CO_2

(99.999%) was supplied by Air Liquide. Elemental analysis was obtained on a Vario EL elemental analyzer. Thermogravimetric analysis (TGA) was carried out in oxygen using a Perkin-Elmer STA 6000 at a heating rate of $10 \text{ K}\cdot\text{min}^{-1}$. IR spectra were acquired on a Varian IR spectrometer equipped with an ATR cell. ^{13}C and $^{15}\text{N}\{^1\text{H}\}$ CP-MAS measurements were carried out using a Bruker Avance 400 spectrometer operating at 100.6 MHz for ^{13}C using a Bruker 4 mm double resonance probe-head operating at a spinning rate of 10 kHz . N_2 sorption analysis was performed at 77 K using a QUADRASORB SI, equipped with automated surface area and pore size analyzer. Before analysis, samples were degassed at $150 \text{ }^\circ\text{C}$ for 12 h . BET surface areas were determined over a $0.05\text{--}0.25 \text{ P/P}_0$ range. CO_2 sorption measurements at 273 K were acquired on an Autosorb 1-MP machine from Quantachrome Instruments. Quantitative analysis of the catalytic tests was conducted by GC-MS, for which an Agilent Technologies 7890 A GC system running with a HP-5 MS capillary column and an Agilent Technologies 5975 C mass selective detector were employed with a known amount of toluene as external standard. X-ray powder diffraction (XRD) patterns were measured in reflection mode ($\text{Cu-K}\alpha$ radiation) on a Bruker D8 diffractometer equipped with scintillation counter. Crystal unit cell model construction and diffraction peaks simulations were done by using Material Studio 4.3 computer program suite. Temperature-programmed desorption (TPD) experiments were conducted on a Quantachrome ChemBET PULSAR instrument. In a typical experiment, 110 mg of sample was placed in a U-shaped, flow-through, quartz sample tube. Before the TPD experiments, the catalyst was pretreated in helium ($50 \text{ cm}^3\cdot\text{min}^{-1}$) at 803 K for 1 h . CO_2 was then passed ($50 \text{ cm}^3\cdot\text{min}^{-1}$) at 298 K for 1 h . The sample was subsequently flushed in helium ($50 \text{ cm}^3\cdot\text{min}^{-1}$) at 298 K for 1 h to remove physisorbed CO_2 . The TPD experiments were carried out from 298 to 803 K at a heating rate of $10 \text{ K}\cdot\text{min}^{-1}$. ICP-OES measurements were conducted in the Fraunhofer Institute für Angewandte Polymerforschung, Golm.

Synthesis. In a typical experiment, a mixture of 2.0 g (13 mmol) of TCB and 1.8 g (13 mmol) of desiccated ZnCl_2 was placed into a quartz ampule and dried in vacuum at $100 \text{ }^\circ\text{C}$ for 12 h . The ampule was then flame-sealed and transferred into a furnace for heat treatment at $400 \text{ }^\circ\text{C}$ and 40 h . After cooling to room temperature, the ampule was broken open, and the solid monolith obtained was ground thoroughly. The powder was washed in hot water ($90 \text{ }^\circ\text{C}$) with vigorous stirring for 12 h . The washing solution was exchanged for 0.1 M HCl , and the powder was further washed at $90 \text{ }^\circ\text{C}$ for another 12 h with vigorous stirring. The solid was finally washed successively with water, DMSO, and acetone and dried in vacuum at $150 \text{ }^\circ\text{C}$ for 12 h .

Caution: For temperatures higher than $500 \text{ }^\circ\text{C}$, the ampules are under pressure, which is released during opening.

Catalytic Tests. The reactor setup consisted of a 100 mL stainless steel Berghof BR-100 high pressure reactor with simple heating and stirring using a laboratory heating plate with heater block. The reactor was fitted with a Teflon insert, a pressure indicator, a temperature probe submersion tube to measure the internal reactor temperature,

Table 1. Reaction Conditions and Porosity of CTF-0 Polymers

entry	ZnCl ₂ (mol equiv)	time (h)	temp (°C)	S _{BET} ^a (m ² ·g ⁻¹)	V _{0.1} ^b (cm ³ ·g ⁻¹)	V _{tot} ^c (cm ³ ·g ⁻¹)	V _{0.1} /V _{tot}	CO ₂ uptake ^d (mmol·g ⁻¹) (wt%)
1	0.5	10	400	412	0.18	0.26	0.69	n.m. ^e
2	1	10	400	546	0.17	0.34	0.50	n.m. ^e
3	1.5	10	400	232	0.05	0.34	0.15	n.m. ^e
4	0.5	40	400	432	0.15	0.26	0.58	n.m. ^e
5	1	40	400	427	0.18	0.29	0.62	1.67 (6.8)
6	1.5	40	400	687	0.28	0.42	0.67	1.54 (6.3)
7	5	40	400	499	0.21	0.47	0.45	2.25 (9.0)
8	1	80	400	-	-	-	-	2.34 (9.3)
9	5	20/20	400/600	2011	0.52	1.53	0.34	4.22 (15.7)

^aSurface area determined by the BET method. ^bV_{0.1} = pore volume calculated at P/P₀ = 0.1. ^cV_{tot} = pore volume calculated at P/P₀ = 0.99. ^dCO₂ uptake measured at 273 K and 1 bar. ^en.m. = not measured.

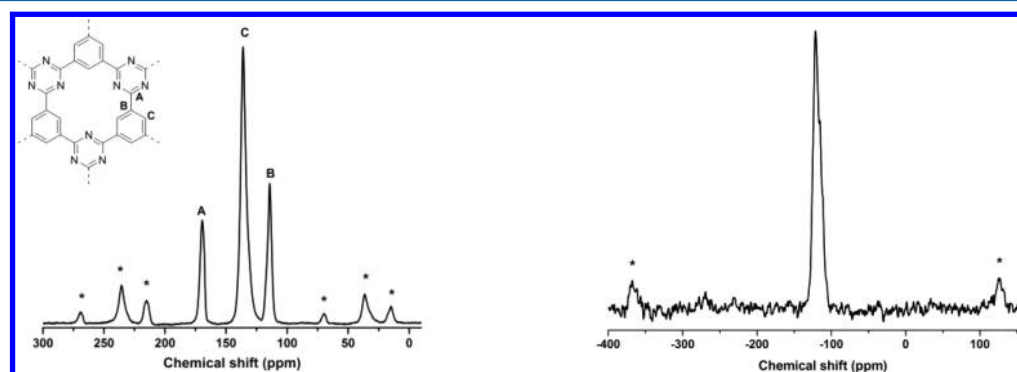


Figure 1. ¹³C CP-MAS solid state NMR (left) and ¹⁵N CP-MAS solid state NMR (right) of CTF-0. Asterisks denote spinning sidebands.

and a pressure relief valve and a metal rupture disc to safely limit the maximum pressure. In a typical reaction, 100 mg of catalyst and 18 mmol of epichlorohydrin were charged in a 100 mL Teflon insert. The reactor was sealed and flushed 5 times at room temperature with CO₂ to remove the air from the vessel. The pressure was adjusted to 6.9 bar, and the reactor was heated to 130 °C. After 4 h reaction time, the reactor was cooled down to room temperature, and the pressure was released. The collected sample was centrifuged, filtered, and analyzed by GC-MS.

RESULTS AND DISCUSSION

Synthesis and Structure of CTF-0. CTF-0 was synthesized under ionothermal conditions in sealed quartz ampules by heating 1,3,5-tricyanobenzene (TCB) in the presence of ZnCl₂. It has been reported that careful adjustment of the reaction conditions is required when 1,4-dicyanobenzene was used as monomer to yield the crystalline framework denoted as CTF-1.³⁰ Notably the monomer to salt ratio was found to be crucial in order to synthesize materials with long-range order. Therefore, we investigated the influence of the amount of ZnCl₂, as well as reaction time and temperature on the properties of the material when TCB was applied as monomer (Samples are denoted as CTF-0-temperature(°C)-time(h)-mol equiv of ZnCl₂, e.g. CTF-0-400-40-1 for a CTF-0 prepared at 400 °C for 40 h with 1 mol equiv of ZnCl₂). The reaction conditions and the chemical and structural characteristics of all the polymerized networks are summarized in Table 1. Black monoliths were obtained directly after synthesis, and the CTFs were collected as brownish powders after grinding and extensive washing to remove ZnCl₂. Just very little amounts of residual zinc were detected using ICP analysis (Figure S1). The polymerization yields were typically >90% suggesting low amounts of side-reactions during the course of the reaction. The successful formation of the polytriazine networks was

indicated by FT-IR analysis (Figure S2). The intensity of the characteristic carbonitrile stretching band of the starting monomer around 2240 cm⁻¹ decreased significantly during the course of the reaction, while the aromatic C–N stretching band characteristic of the tri-s-triazine units at 1520 and 1310 cm⁻¹ appeared for all the synthesized networks, even after 10 h reaction time. Notably the IR spectra of CTF-0-400-x-1 did not change considerably when 10, 40, or 80 h reaction time was applied, even though further analysis (see below) showed significant changes in the structure of the networks. This suggests that extended frameworks were already formed after short reaction times, while in the further course of the reaction, the reversible opening and closing of triazine rings resulted to the final crystalline structure. Elemental analysis showed just a small deviation from the theoretical C/H/N values for all samples as typically observed for highly cross-linked polymers, due to incomplete combustion and adsorbed moisture (Table S1). Notably the C/H/N values are nearly unchanged when different monomer/ZnCl₂ ratios or longer reaction times are applied. Even after 80 h reaction at 400 °C the C/N ratio stayed close to the expected values, showing the high chemical and thermal stability of the networks once formed. To further prove the thermal stability of CTF-0 thermogravimetric analysis (TGA) was carried out. CTF-0 proved to be even more stable than CTF-1 i.e. thermally stable in oxygen atmosphere up to 600 °C (Figure S3). The higher thermal stability could be attributed to the higher nitrogen content and the higher cross-linking density in the material in comparison to CTF-1. It should be noted that the thermal stability of most microporous polymers and COFs is much lower and in most cases only TGA measurements under inert gas are reported. Thus the TGA measurements under oxygen supported again the impressive stability of CTFs under realistic conditions.

^{13}C CP-MAS solid state NMR (Figure 1) confirmed the almost complete trimerization of the starting monomer. Indeed besides the three expected peaks at $\delta = 167$, 136, and 114 ppm attributed to the three sp^2 carbons of the ideal CTF-0 framework, no peaks of residual cyano groups (110 ppm) could be detected in the spectrum. Furthermore ^{15}N solid state NMR (Figure 1) of the framework proved that nitrogen was just present in the form of triazine rings as one single peak at a chemical shift of $\delta = -121$ ppm was observed which could be assigned to the triazine moiety.³⁸

The porous structure of the resulting CTFs was investigated by N_2 sorption experiments at 77 K (Table 1, Figure 2). All the

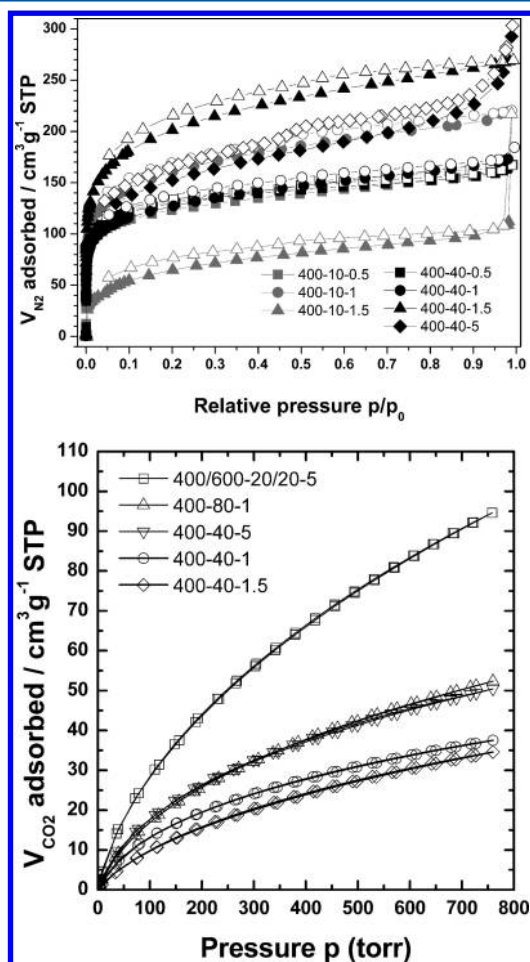


Figure 2. N_2 sorption isotherms (filled symbols indicate adsorption branches and open symbols indicate desorption branches) measured at 77 K (top). CO_2 adsorption/desorption isotherms measured at 273 K (bottom).

samples synthesized at 400 °C showed type I isotherms indicative of microporous materials with apparent BET surface areas ranging from 232 to 687 $\text{m}^2 \cdot \text{g}^{-1}$. In general the specific surface area varied in a range between 400 and 550 $\text{m}^2 \cdot \text{g}^{-1}$. However, the polymerization of this trisubstituted monomer into an ideal framework (see Scheme 1 and the SI) should give rise to a comparably dense organic network with very small pores, and therefore low or even no detectable surface area would be expected from nitrogen sorption measurement. The assumption was confirmed by modeling⁴¹ of the ideal CTF-0 eclipsed structure, which predicts the solvent accessible surface area of the network to be 0 $\text{m}^2 \cdot \text{g}^{-1}$, as the pore entrances are

too narrow to allow the uptake of a probe with a radius of 1.82 Å (N_2) (Figure S5). Therefore it can be assumed that the presence of defects within the structure is the origin of the observed, still significant porosity. However, comparing the samples polymerized at 400 °C with 1 mol equiv of ZnCl_2 but applying different reaction times revealed a decrease in surface area from 546 $\text{m}^2 \cdot \text{g}^{-1}$ after 10 h to 427 $\text{m}^2 \cdot \text{g}^{-1}$ after 40 h to no accessible surface area after 80 h (Table 1, entries 2, 5, and 8). It can thus be assumed that longer reaction times yield materials with increasing crystallinity, and, finally, after 80 h reaction, the expected dense material is formed with pores not accessible to nitrogen. On the other hand, as expected, very high surface area ($\sim 2000 \text{ m}^2 \cdot \text{g}^{-1}$) could be reached by conducting the polymerization at higher temperature (Table 1, entry 9). This result is in line with previous reports, in which very high surface areas were reported for various dicyanomonomomers however at the cost of crystallinity and the formation of larger defect sites seen in a strong depletion of the nitrogen content (see Table S1).^{32,33} However, due to the high amount of nitrogen in the CTF-0 precursor also in the high surface area material still considerable amounts of nitrogen (19.3 wt %) are found.

The carbon dioxide uptakes of selected networks were measured. An uptake of 4.22 $\text{mmol} \cdot \text{g}^{-1}$ (15.7 wt %) was observed for the high surface area network, which is in the range of the highest values observed for organic polymers under these conditions.⁶ Also the other polymer networks adsorb significant amounts of CO_2 even though the uptakes were comparably lower due to the overall lower surface area. Notably, the highest CO_2 uptake of 2.34 $\text{mmol} \cdot \text{g}^{-1}$ (9.3 wt %) within this series was observed from the polymer network synthesized for 80 h, which showed no accessibility to N_2 . Thus a high selectivity of CO_2 over N_2 can be assumed for CTF-0-400-80-1.

It should be noted that from Figure S5 an ideal CTF-0 should not only exclude N_2 but also CO_2 due to the small pore openings. Therefore it can be assumed that also CTF-0-400-80-1 still features enough defect sites to at least accommodate CO_2 , while it is already dense enough to exclude N_2 . Of course also the different measurement conditions for N_2 and CO_2 sorption have to be taken into account.

PXRD measurements (Figure 3) showed that all the resulting materials were at least partially crystalline, while the intensity

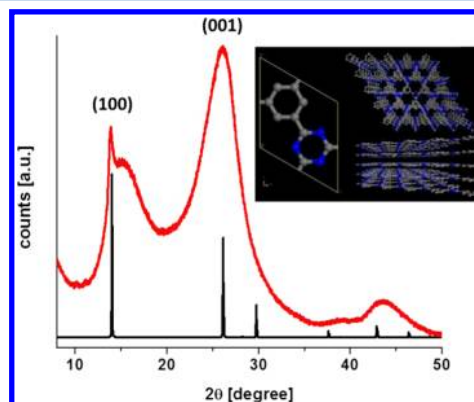


Figure 3. PXRD patterns of CTF-0-400-80-1. For comparison a simulated pattern of an ideal CTF-0 structure is shown assuming an eclipsed stacking of the sheets and unit cell parameters of $a = b = 7.3 \text{ Å}$ and $c = 3.3 \text{ Å}$ (inset).

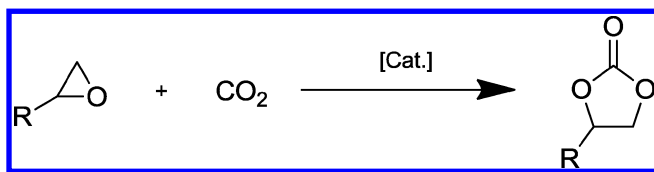
and width of the peaks could be influenced by the monomer/ ZnCl_2 ratio and reaction time and temperature. In all samples two distinct peaks at 14° and 26° could be distinguished.

Even though these peaks were too broad to give a conclusive picture on the atomistic structure of the frameworks the low-angle peak could be interpreted as the in-plane reflection (100) of the ideal structure (Table S2, Figure S4), while the broad (001) diffraction peak at $\sim 26^\circ$ could be attributed to a vertical spacing between stacked sheets of 3.35 Å. In all patterns (Figure S6) a broad shoulder close to the rather sharp low angle peaks assigned to the in-plane (100) reflection was observed. In fact, all the XRD patterns give the impression that higher and lower organized fractions of the networks can be found in the samples, whose diffraction patterns are superimposed in the measurements. Assuming stacking of the triazine connected sheets, for the ideal CTF-0, a unit cell belonging to the $P6$ space group with unit cell parameters of $a = b = 7.3$ Å and $c = 3.3$ Å could be deduced. The layers of CTF-0 sheets could be stacked in an eclipsed and staggered fashion, while the XRD patterns do not clearly support one of the possibilities (Figure S7). It should be however noted that calculations on the stacking possibilities of the sheet in two-dimensional COFs also revealed other possibilities.⁴²

Additional sharp diffraction peaks at 5.1° , 5.5° and 10.2° , 11.0° are observed for some samples which possibly belong to the same set of crystallographic planes (Figure S8, Table S3). These peaks were still observed e.g. for CTF-0-400-40-1 even after several reproductions. To the best of our knowledge, these sharp diffraction peaks could not be assigned to any crystal space group involving the ideal structure of CTF-0. Notably, the peaks could be explained assuming a regular pattern of coordinated Zn^{2+} ions within the structure, thus forming a larger $P6$ hexagonal unit cells as illustrated in Figure S9 a and b. However, a higher amount of zinc chloride should be present in order to support this assumption. There was no direct evidence that such regular distribution of Zn in the CTF structures could possibly occur.

CTF-0 as Catalyst. It was recently shown that the high number of basic nitrogen sites in CTF frameworks can efficiently activate and convert CO_2 .³⁹ Thus CTFs were reported to catalyze the formation of cyclic carbonates via the cycloaddition of CO_2 to different epoxides (Scheme 2). It was

Scheme 2. Synthesis of Cyclic Carbonates via Cycloaddition of CO_2 to Epoxides



observed that the chemical and structural properties, namely the amount and type of nitrogen functionalities and the porous characteristics of the frameworks, had significant influence on the catalytic performance of the materials.

Selected samples from the CTF-0 series were tested in the demonstrative cyclic chloropropene carbonate formation starting from CO_2 and epichlorohydrin (Scheme 2, $\text{R} = \text{CH}_2\text{Cl}$) and compared to reported CTF-1 samples (Table 2). For clarity reasons the important sample characteristics for the catalytic performance such as N-content, surface area, and pore volume are additionally reported in the table.

In general CTF-0s were catalyzing this reaction under relatively mild, solventless conditions. Indeed, compared to a blank experiment where just a little conversion was observed (2.3%), most CTF-0s showed increased conversion. However, the crystalline CTF-0 showed rather low activity compared to crystalline CTF-1 (entries 2 and 3 vs entry 5). Here, the pore size might be the controlling factor. In this case, the small micropores accommodate CO_2 , as seen from the CO_2 sorption measurements, but do not allow access of the larger epichlorohydrin. Indeed when the surface area and pore size increased, a significant increase in the catalytic activity of CTF-0 was observed, yielding 100% conversion with 92% selectivity after 4 h reaction (Table 2, entry 4). The results are in good accordance with the high activity of the high surface area CTF-1 (Table 2, entry 6), where the presence of additional mesoporosity proved to be beneficial. Furthermore recycling tests proved the stability of the catalyst, and the reaction could be conducted for at least 4 consecutive runs without significant loss of activity (Figure 4). CO_2 thermally programmed desorption (Figure S10) was carried out to yield insights into the basic sites of the materials. Two desorption peaks are observed for CTF-0-400-40-1.5 and CTF-0-400/600-20/20-5. In general, the peaks for the former, low surface area material have much less intensity, in accordance to the lower amount of CO_2 which can be stored in this sample. For both materials a desorption peak at 85°C suggests the presence of weak basic sites, for example triazine moieties on the outer surface. Furthermore a broad and more intense desorption peak at 250 and 290°C , respectively, is found for the materials, which can be attributed to CO_2 chemisorbed within the pores of the materials, thus probably even interacting with more than one basic nitrogen site. The TPD profile of CTF-0-400/600-20/20-5 is similar to that of high surface area CTF-1,³⁹ indicating there is no drastic change in the type of basic sites between the two materials.

CONCLUSIONS

In conclusion, novel covalent triazine frameworks (CTF-0) have been synthesized by the trimerization of 1,3,5-tricyanobenzene. The porosity and structure of the frameworks were influenced by the monomer/ ZnCl_2 ratio, the reaction temperature, and time. Extended frameworks could already be formed after very short reaction times, while in the further course of the reaction, the reversible opening and closing of triazine rings resulted to the final crystalline structure. Thus, while the chemical composition was not affected by various reaction times, the porosity and structure were greatly influenced. Thus after 80 h reaction time a framework was formed, which showed no porosity according to nitrogen sorption measurements as would be expected from the very small pores formed by an ideal CTF-0 framework. However XRD measurements revealed that some amorphous fractions coexisted with the crystalline fractions. Unfortunately, the amount of these two phases could not be easily quantified. The less ordered parts might also be responsible for the high uptake of CO_2 in contrast to N_2 . Thus in principle it is difficult to differentiate between the porosity which arise from the hexagonal channels of an ordered framework and the residual pores formed by a less ordered, probably defective network. This study however reveals that the latter contribution can be considerable. However, in other cases like the much more ordered COFs and CTF-1 indeed the crystalline parts will mainly contribute to the overall surface area.

Table 2. Structural Parameters and Catalytic Performance of Various CTFs in the Formation of Chloropropene Carbonate from CO₂ and Epichlorohydrin^g

entry	catalyst	N ^a (%)	S _{BET} ^b (m ² ·g ⁻¹)	V _p ^c (cm ³ ·g ⁻¹)	conversion ^d (%)	selectivity ^d (%)
1	blank	-	-	-	2.3	n.d. ^e
2	CTF-0-400-40-1	22.3	427	0.29	4.3	n.d. ^e
3	CTF-0-400-40-1.5	22.0	687	0.42	20.4	87.7
4	CTF-0-400/600-20/20-5	19.3	2011	1.53	100	92.6
5	CTF-1 ^f	19.7	536	0.38	81.2	94.4
6	CTF-1-HSA ^f	8.8	2087	1.30	100	95.8

^aDetermined from elemental analysis. ^bSurface area determined by the BET method. ^cV_p = pore volume calculated at P/P₀ = 0.99. ^dDetermined by GC-MS. ^eNot determined. ^fValues from ref 39. ^gSee Scheme 2, R = CH₂Cl. Reactions conditions: 18 mmol epichlorohydrin, 100 mg catalyst, 130 °C, 6.9 bar CO₂, 4 h, without solvent.

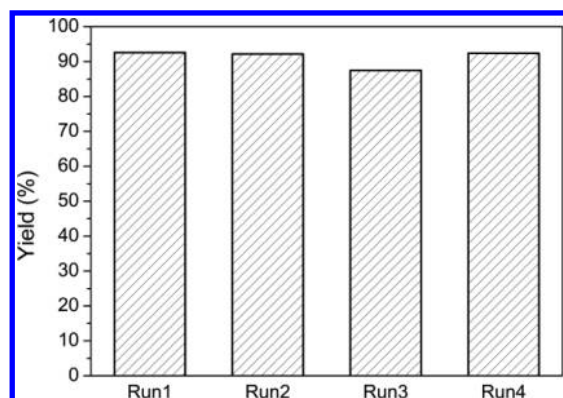


Figure 4. Catalytic yields of CTF-0-400/600-20/20-5 in the chloropropene carbonate formation upon recycling (reactions conditions: 18 mmol epichlorohydrin, 100 mg catalyst, 130 °C, 6.9 bar CO₂, 4 h, without solvent).

An amorphous framework with surface areas as high as 2000 m²·g⁻¹ was observed when the final reaction temperature was increased to 600 °C. This material however showed still a very high amount of nitrogen atoms (19.3 wt %) in the framework. Due to its high surface areas and nitrogen content this framework showed exceptional uptake of CO₂ and is a suitable metal-free catalyst for formation of cyclic carbonates from CO₂ and epoxides.

■ ASSOCIATED CONTENT

Supporting Information

TGA curves, elemental analysis results, ICP measurements, FT-IR measurements, chemisorption measurements, fractional atomic coordinates of an ideal CTF-0 unit cell, XRD measurements, XRD fittings from differently modeled CTF-0 stacking possibilities, and illustrated assumption about the reason for sharp peaks at lower angles from XRD measurements for crystalline CTF-0. This material is available free of charge via the Internet at <http://pubs.acs.org>.

■ AUTHOR INFORMATION

Corresponding Author

*E-mail: arne.thomas@tu-berlin.de.

Notes

The authors declare no competing financial interest.

■ ACKNOWLEDGMENTS

Financial support of the German Federal Ministry of Education and Research, BMBF (project “Dream Reactions” (01RC0901F)), the German Science Foundation, DFG

(project TH1463/2-1) and the Cluster of Excellence “Unifying Concepts in Catalysis” (EXL 31411) is highly acknowledged.

■ REFERENCES

- (1) Schueth, F.; Sing, K. S. W.; Weitkamp, J. *Handbook of Porous Solids*; Wiley VCH: Weinheim, 2002.
- (2) Cheetham, A. K.; Ferey, G.; Loiseau, T. *Angew. Chem., Int. Ed.* **1999**, *38*, 3268.
- (3) Kitagawa, S.; Kitaura, R.; Noro, S. *Angew. Chem., Int. Ed.* **2004**, *43*, 2334.
- (4) Yaghi, O. M.; O’Keeffe, M.; Ockwig, N. W.; Chae, H. K.; Eddaoudi, M.; Kim, J. *Nature* **2003**, *423*, 705.
- (5) Thomas, A. *Angew. Chem., Int. Ed.* **2010**, *49*, 8328.
- (6) Dawson, R.; Cooper, A. I.; Adams, D. J. *Prog. Polym. Sci.* **2012**, *37*, 530.
- (7) McKeown, N. B.; Budd, P. M. *Chem. Soc. Rev.* **2006**, *35*, 675.
- (8) Thomas, A.; Goettmann, F.; Antonietti, M. *Chem. Mater.* **2008**, *20*, 738.
- (9) Weber, J.; Antonietti, M.; Thomas, A. *Macromolecules* **2008**, *41*, 2880.
- (10) Tsyurupa, M. P.; Davankov, V. A. *React. Funct. Polym.* **2002**, *53*, 193.
- (11) Tsyurupa, M. P.; Davankov, V. A. *React. Funct. Polym.* **2006**, *66*, 768.
- (12) Cooper, A. I. *Adv. Mater.* **2009**, *21*, 1291.
- (13) Jiang, J.-X.; Su, F.; Trewin, A.; Wood, C. D.; Campbell, N. L.; Niu, H.; Dickinson, C.; Ganin, A. Y.; Rosseinsky, M. J.; Khimyak, Y. Z.; Cooper, A. I. *Angew. Chem., Int. Ed.* **2007**, *46*, 8574.
- (14) McKeown, N. B.; Budd, P. M.; Msayib, K. J.; Ghanem, B. S.; Kingston, H. J.; Tattershall, C. E.; Makhseed, S.; Reynolds, K. J.; Fritsch, D. *Chem.—Eur. J.* **2005**, *11*, 2610.
- (15) Schmidt, J.; Weber, J.; Epping, J. D.; Antonietti, M.; Thomas, A. *Adv. Mater.* **2009**, *21*, 702.
- (16) Schmidt, J.; Werner, M.; Thomas, A. *Macromolecules* **2009**, *42*, 4426.
- (17) Weber, J.; Thomas, A. *J. Am. Chem. Soc.* **2008**, *130*, 6334.
- (18) Côté, A. P.; Benin, A. I.; Ockwig, N. W.; O’Keeffe, M.; Matzger, A. J.; Yaghi, O. M. *Science* **2005**, *310*, 1166.
- (19) El-Kaderi, H. M.; Hunt, J. R.; Mendoza-Cortes, J. L.; Côté, A. P.; Taylor, R. E.; O’Keeffe, M.; Yaghi, O. M. *Science* **2007**, *316*, 268.
- (20) Feng, X.; Ding, X.; Jiang, D. *Chem. Soc. Rev.* **2012**, *41*, 6010.
- (21) Mastalerz, M. *Angew. Chem., Int. Ed.* **2008**, *47*, 445.
- (22) Bojdys, M. J.; Wohlgemuth, S. A.; Thomas, A.; Antonietti, M. *Macromolecules* **2010**, *43*, 6639.
- (23) Cote, A. P.; El-Kaderi, H. M.; Furukawa, H.; Hunt, J. R.; Yaghi, O. M. *J. Am. Chem. Soc.* **2007**, *129*, 12914.
- (24) Dogru, M.; Sonnauer, A.; Gavryushin, A.; Knochel, P.; Bein, T. *Chem. Commun.* **2011**, *47*, 1707.
- (25) Spitler, E. L.; Dichtel, W. R. *Nat. Chem.* **2010**, *2*, 672.
- (26) Tilford, R. W.; Gemmill, W. R.; zur Loye, H. C.; Lavigne, J. J. *Chem. Mater.* **2006**, *18*, 5296.
- (27) Uribe-Romo, F. J.; Hunt, J. R.; Furukawa, H.; Klock, C.; O’Keeffe, M.; Yaghi, O. M. *J. Am. Chem. Soc.* **2009**, *131*, 4570.

- (28) Wan, S.; Guo, J.; Kim, J.; Ihee, H.; Jiang, D. L. *Angew. Chem., Int. Ed.* **2008**, *47*, 8826.
- (29) Wan, S.; Guo, J.; Kim, J.; Ihee, H.; Jiang, D. L. *Angew. Chem., Int. Ed.* **2009**, *48*, 5439.
- (30) Kuhn, P.; Antonietti, M.; Thomas, A. *Angew. Chem., Int. Ed.* **2008**, *47*, 3450.
- (31) Kuhn, P.; Forget, A.; Hartmann, J.; Thomas, A.; Antonietti, M. *Adv. Mater.* **2009**, *21*, 897.
- (32) Kuhn, P.; Forget, A.; Su, D.; Thomas, A.; Antonietti, M. *J. Am. Chem. Soc.* **2008**, *130*, 13333.
- (33) Kuhn, P.; Thomas, A.; Antonietti, M. *Macromolecules* **2009**, *42*, 319.
- (34) Bojdys, M. J.; Jeromenok, J.; Thomas, A.; Antonietti, M. *Adv. Mater.* **2010**, *22*, 2202.
- (35) Chan-Thaw, C. E.; Villa, A.; Katekomol, P.; Su, D. S.; Thomas, A.; Prati, L. *Nano Lett.* **2010**, *10*, 537.
- (36) Chan-Thaw, C. E.; Villa, A.; Prati, L.; Thomas, A. *Chem.—Eur. J.* **2011**, *17*, 1052.
- (37) Palkovits, R.; Antonietti, M.; Kuhn, P.; Thomas, A.; Schüth, F. *Angew. Chem., Int. Ed.* **2009**, *48*, 6909.
- (38) Hug, S.; Tauchert, M. E.; Li, S.; Pachmayr, U. E.; Lotsch, B. V. *J. Mater. Chem.* **2012**, *22*, 13956.
- (39) Roeser, J.; Kailasam, K.; Thomas, A. *ChemSusChem* **2012**, DOI: 10.1002/cssc.201200091.
- (40) Ren, S.; Bojdys, M. J.; Dawson, R.; Laybourn, A.; Khimyak, Y. Z.; Adams, D. J.; Cooper, A. I. *Adv. Mater.* **2012**, *24*, 2357.
- (41) Trewin, A.; Cooper, A. I. *CrystEngComm* **2009**, *11*, 1819.
- (42) Lukose, B.; Kuc, A.; Heine, T. *Chem.—Eur. J.* **2011**, *17*, 2388.